Synthetic quorum sensing in model microcapsule colonies

Henry Shum[a,1] and Anna C. Balazs[a,2]

[a]Department of Chemical & Petroleum Engineering, University of Pittsburgh, Pittsburgh, PA 15261

Edited by Andrea J. Liu, University of Pennsylvania, Philadelphia, PA, and approved June 30, 2017 (received for review February 10, 2017)

Biological quorum sensing refers to the ability of cells to gauge their population density and collectively initiate a new behavior once a critical density is reached. Designing synthetic materials systems that exhibit quorum sensing-like behavior could enable the fabrication of devices with both self-recognition and self-regulating functionality. Herein, we develop models for a colony of synthetic microcapsules that communicate by producing and releasing signaling molecules. Production of the chemicals is regulated by a biomimetic negative feedback loop, the "repressilator" network. Through theory and simulation, we show that the chemical behavior of such capsules is sensitive to both the density and number of capsules in the colony. For example, decreasing the spacing between a fixed number of capsules can trigger a transition in chemical activity from the steady, repressed state to large-amplitude oscillations in chemical production. Alternatively, for a fixed density, an increase in the number of capsules in the colony can also promote a transition into the oscillatory state. This configuration-dependent behavior of the capsule colony exemplifies quorum-sensing behavior. Using our theoretical model, we predict the transitions from the steady state to oscillatory behavior as a function of the colony size and capsule density.

quorum sensing | repressilator | microcapsules

Quorum sensing (QS) refers to the ability of organisms in a population to assess the number and density of individuals present, allowing a specific behavior to be initiated only when a critical threshold in the population size and density is reached. QS plays a vital role in the life cycle of bacteria (1, 2), yeast (3, 4), and slime molds (5, 6), as well as social insects (7). In microorganisms, QS is based on chemical signaling among individuals in a colony. Bacteria (1, 8), for example, produce and secrete signaling molecules, which diffuse into the surrounding medium where they can be detected by other cells in the population. Through regulatory networks, the signaling molecule acts as an autoinducer; the rate of production of the autoinducer increases with its concentration. When the cell density is low, the concentration of the signaling molecule is low, and production is maintained at a low, basal rate. The cells are considered to be in the "off" QS state. When the population density is high, each cell detects a high concentration of the signaling molecule resulting from the collective production of many nearby neighbors. The cells are switched "on," increasing production of the signaling molecule and activating further metabolic pathways that are triggered by QS. Hence, spatially separated cells interact through regulatory networks, which coordinate the collective behavior of the colony.

An intriguing challenge in both synthetic biology and materials science is to design man-made systems that exhibit behavior analogous to QS, i.e., sensing and responding to the system size and density. Such synthetic QS abilities could provide a route to creating materials and devices with novel self-recognition and self-regulating functionality. Namely, elements in these materials systems would effectively "count" and only operate when the number of neighboring elements becomes sufficiently high. For example, a soft material with embedded QS elements could switch on a certain chemical behavior when compressed and switch off when stretched.

Several mathematical models of the autoinducer system have been developed to describe how the switch from the off to the on state is controlled in bacterial QS (9–11). Common to these models is the existence of multiple steady states such that a change in the concentration of external signaling molecules leads to a sudden jump from a low production state to a high production state. The resulting QS transition is hysteretic; the cell density at which the population switches on is higher than the density at which the population switches off. This hysteresis prevents the colony from rapidly alternating between on and off states in the presence of small fluctuations, thus stabilizing the population behavior.

To accurately detect the population density in a synthetic materials system, however, the existence of two stable states leads to ambiguity, as the behavior of the system would depend on the history of past states. A potential solution to this problem, allowing self-regulating materials to uniquely determine the present density, is to use a different regulatory network known as the "repressilator," which exhibits a single steady state. The repressilator circuit (12) consists of a cycle of three genes that code for the repressors of the next gene in the cycle, and thus the whole system operates through an engineered negative feedback loop. Under the repressilator, chemical "c_1" suppresses the production of chemical "c_2," which suppresses the production of chemical "c_3," which in turn suppresses the production of "c_1." The repressilator was engineered as an artificial gene network in *Escherichia coli* cells, resulting in oscillations in the production of a specific protein (12).

Mathematical models for chemical production regulated by the repressilator network have shown that the long-term behavior of the network is either stationary or oscillatory, depending on system parameters (12–15). Associating the stationary behavior with an off state and oscillatory behavior with an on state, the

Significance

Many organisms, from bacteria to humans, can sense their local population density and modify their behavior in crowded environments. This density-dependent behavior, known as quorum sensing, is a highly desirable attribute for synthetic systems because it permits novel self-recognition and self-regulating functionality. Using theory and simulation, we design chemical-producing microcapsules that display quorum sensing. When the chemical production is regulated by a biomimetic feedback loop, the capsules exhibit tunable transitions between steady ("off") and oscillatory ("on") states as a function of the number and number density of microcapsules in a colony. Such a system can behave as a mechanoresponsive material, modulating chemical activity when applied stresses alter the spatial configuration of the capsules.

Author contributions: H.S. and A.C.B. designed research; H.S. performed research; H.S. and A.C.B. analyzed data; and H.S. and A.C.B. wrote the paper.

The authors declare no conflict of interest.

This article is a PNAS Direct Submission.

[1]Present address: Department of Applied Mathematics, University of Waterloo, Waterloo, ON, Canada N2L 3G1.

[2]To whom correspondence should be addressed. Email: balazs@pitt.edu.

This article contains supporting information online at www.pnas.org/lookup/suppl/doi:10.1073/pnas.1702288114/-/DCSupplemental.

repressilator network could support QS ability if the emergent state depended on the population density. Prior models (12–15), however, described the dynamics of small systems in which spatial variations in concentrations are unimportant, such as within a single cell or tightly packed cluster of a few cells. Hence, these models cannot reveal how changes in colony size and number density could lead to oscillations and, ultimately, QS.

It is known that oscillatory reactions can lead to complex dynamical behavior, including the emergence of traveling waves, in large colonies of chemically communicating cells (16) or continuous reactive media (17). Moreover, studies of systems at intermediate sizes, such as a growing colony of bacteria (18) and clusters of ∼100 catalytic particles in an excitable medium (19), have demonstrated that oscillatory networks can endow a system with QS characteristics; oscillations emerge and become synchronized only when a critical density and number of agents is reached. Theoretical understanding of the conditions required for oscillations in such systems, however, is lacking. Specifically, it remains unclear what combinations of numbers and densities of agents allow a "quorum" to be reached (as indicated by the presence of sustained oscillations) for a given regulatory network and set of physical and chemical parameters.

As a route to addressing these questions and thereby articulating necessary conditions for QS in a synthetic system, we model the dynamics in a colony of immobile microcapsules that release diffusible signaling chemicals into the surrounding fluid. We consider the production of these signaling chemicals to be regulated by an abstraction of the repressilator feedback network; namely, we do not model the biochemical pathways of a genetic repressilator circuit but simply consider three chemical species that follow the cycle of inhibition prescribed by the repressilator network. Adopting the generalized definition of QS as a qualitative switch in the behavior of the system with a change in the size and density of a colony, we numerically determine conditions under which colonies of capsules achieve a quorum, characterized by sustained chemical oscillations in the repressilator network. As described in *Results and Discussion*, we find that there is a critical colony radius below which a quorum is not reached. By tuning the reaction kinetics, it is also possible to quench oscillations in large colonies, so that only colonies within a specific range of sizes become activated. Finally, at the end of *Conclusions*, we allude to recent experimental studies that can facilitate the physical realization of this synthetic QS system.

Results and Discussion

The Discrete Capsule Model. We model the colony of microcapsules as a set of regions in space where the production of chemicals is regulated by the repressilator feedback network. The number of capsules in the colony is N_{cap}, and the position of the capsule with index k is $\mathbf{X}^k$, $k=1,2,3,\ldots,N_{cap}$. Although arbitrary arrangements of the capsules can be studied with this model, we focus on random, uniformly distributed capsules in a circular disk-shaped region of radius R_{col} confined between parallel walls with separation h, as illustrated in Fig. 1*A*. Each capsule is a 3D sphere of radius R_{cap} containing enzymes that produce the signaling chemicals (Fig. 1*B*). The capsule's shell is selectively permeable; it prevents the enzymes from leaving the capsule but allows the reactants and products of the enzymatic reaction to freely diffuse into and out of the shell. Assuming that the reactants are always in excess, the rates of reaction can be taken to be independent of reactant concentrations. Hence, we do not explicitly model nor further discuss the reactants. It is the products that are of interest, because they act as signaling species in our system.

With the repressilator (12–14) modulating the production of signaling species in the capsule, species j, with concentration denoted by c_j, acts as an inhibitor for the production of the next chemical $j+1$ in the cycle, and, conversely, the production of species j is inhibited by the presence of chemical $j-1$ (Fig. 1*B*). (The indices referring to chemical species are interpreted modulo 3.) Treating the enzyme as a uniformly distributed continuum within the capsules, the rates of production per unit volume p_j^{cap} depend on the local concentrations c_j as

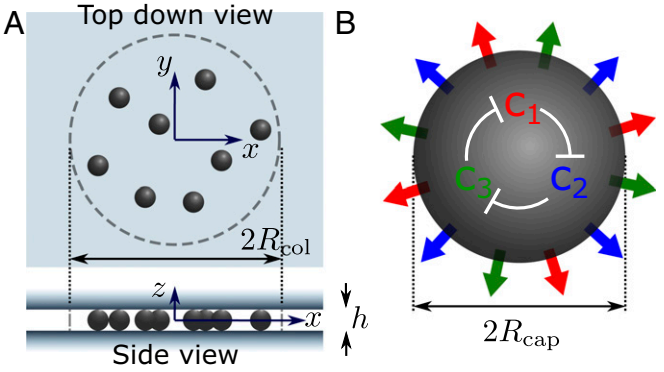

Fig. 1. Schematic diagram of model capsules and colony. (*A*) Top-down and side views of the colony geometry. Capsules are distributed randomly within a disk of radius R_{col} and confined within a height h (the separation between the parallel plates). (*B*) Depiction of a capsule that produces and releases chemicals into the surroundings. Three chemical species are produced with rates modulated by the repressilator network, which is indicated schematically in the center of the capsule. The bar-headed arrow represents inhibition, so that chemical c_1 inhibits the production of c_2, c_2 inhibits the production of c_3, and c_3 inhibits the production of c_1.

$$p_j^{cap} = f(c_{j-1}), \quad j=1,2,3, \qquad [1]$$

where f is a function describing the effect of the inhibitor. As in previous theoretical studies of repressilator systems (12–14), we model inhibition using the Hill function (20). Expressed in dimensionless form (see *SI Text* for details of nondimensionalization), the Hill function reads $f(c)=p^{max}/(1+c^n)$, where p^{max} is the maximum production rate per unit volume; for brevity, we also refer to p^{max} as the "production capacity." Experimentally, this quantity would depend on the concentration of enzymes in the capsules and the maximum turnover rate for the enzymes. The parameter n, known as the Hill coefficient or cooperativity, characterizes the sharpness of the transition from the unrepressed state (no inhibitor present) to the repressed state (high inhibitor concentration). Our model assumes identical kinetic parameters p^{max} and n for the production of all three species within the capsule; the model can, however, be extended to accommodate different production capacities or inhibitor cooperativities for each species.

In addition to production, each signaling species undergoes first-order degradation and diffuses throughout a laterally (x,y) unbounded domain. The nondimensionalized reaction–diffusion equations, boundary conditions, and initial conditions for the concentration fields are given by

$$\partial_t c_j(\mathbf{x},t) = \nabla^2 c_j(\mathbf{x},t) - c_j(\mathbf{x},t) + p_j(\mathbf{x},t), \quad j=1,2,3, \qquad [2]$$

$$\left.\frac{\partial c_j}{\partial z}\right|_{z=-h/2} = \left.\frac{\partial c_j}{\partial z}\right|_{z=h/2} = 0, \quad c_j(\mathbf{x},t=0) = c_j^0(\mathbf{x}), \qquad [3]$$

where the production terms are $p_j(\mathbf{x},t) = \sum_{k=1}^{N_{cap}} f[c_{j-1}(\mathbf{x},t)]\Omega_{cap}(\mathbf{x}-\mathbf{X}^k)$. The capsule indicator function,

$$\Omega_{cap}(\mathbf{x}) = \begin{cases} 1, & \text{if } \sqrt{x^2+y^2+z^2} \le R_{cap}, \\ 0, & \text{otherwise}, \end{cases} \qquad [4]$$

restricts the production terms to act only within the capsules. We emphasize that there is no physical boundary around the colony, so the chemicals produced by the capsules are free to diffuse out

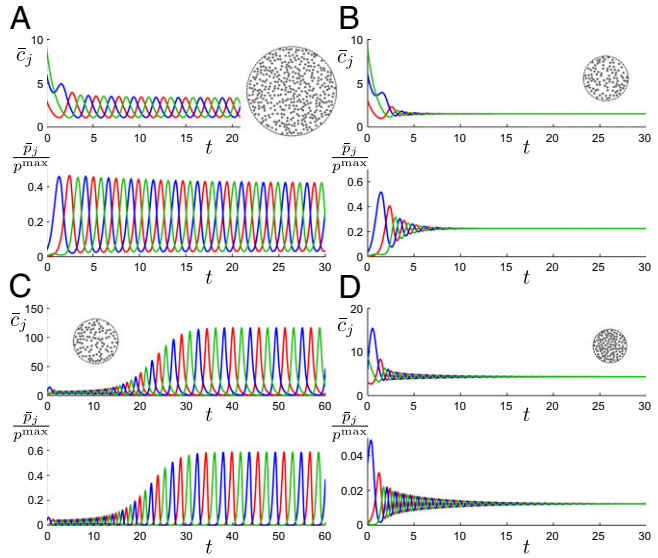

Fig. 2. Average chemical concentrations and production rates over time in different colonies of capsules. Parameters used are (*A*) $N_{cap} = 400$, $p^{max} = 125$, and $R_{col} = 2$; (*B*) $N_{cap} = 100$, $p^{max} = 125$, and $R_{col} = 1$; (*C*) $N_{cap} = 100$, $p^{max} = 5{,}000$, and $R_{col} = 1$; and (*D*) $N_{cap} = 100$, $p^{max} = 5{,}000$, and $R_{col} = 0.75$. In each case, shown are (*Upper*) the average chemical concentrations throughout the colony as functions of time, and (*Lower*) the average production rates normalized by the maximum capacity. A scale representation of each colony is given for visual comparison of colony size and capsule density.

of the colony. It has been argued that bacterial QS is, in fact, based on sensing the rate of diffusion or "leakage" of the signal away from cells (21). Confining the colony in an enclosed space would alter the behavior of the system and negate potential influences of colony size.

We numerically solve the reaction–diffusion equations using a finite difference method (*Methods*). There are five model parameters: Hill coefficient n, production capacity p^{max}, capsule number N_{cap}, capsule size R_{cap}, and colony size R_{col}. The physical interpretation of dimensionless lengths is discussed in *SI Text*. Fixing the Hill coefficient to $n = 3$ and the capsule size to $R_{cap} = 0.05$, we observe qualitatively different behavior, depending on the values of the other parameters. With a large number of capsules ($N_{cap} = 400$) of production capacity $p^{max} = 125$ in a large colony of radius $R_{col} = 2$, sustained temporal oscillations emerge in the chemical productions and concentrations (Fig. 2*A*). The amplitudes of these oscillations are all comparable, and the three species oscillate out of phase with each other.

Conversely, when the colony size is decreased while keeping the same number density of capsules ($N_{cap} = 100$, $R_{col} = 1$), the system exhibits transient oscillations, but the concentration fields and production rates rapidly approach a steady state (Fig. 2*B*). The change in capsule activity between sustained oscillatory chemical production in large colonies and steady, or quiescent, production in small colonies exemplifies the QS characteristic of our system.

To determine whether the production capacity affects the behavior of the system, we increase the maximum production rate per unit volume of the capsules from $p^{max} = 125$ to $p^{max} = 5{,}000$. The small colony ($N_{cap} = 100$, $R_{col} = 1$) now exhibits sustained oscillations (Fig. 2*C*). This finding is consistent with our theoretical understanding of the corresponding well-mixed repressilator system, which is known to exhibit oscillations when p^{max} exceeds a critical value (dependent on other parameters) (14). Increasing the number density of capsules should similarly favor oscillations, because chemicals can be produced at a higher rate per unit volume of the colony. Interestingly, however, this is not always the case. For example, when we maintain the same number of capsules and production capacity as in the oscillatory case of Fig. 2*C*, but increase the number density by reducing the radius of the colony from $R_{col} = 1$ to $R_{col} = 0.75$, the capsules no longer sustain oscillations in chemical production and return to the quiescent state (Fig. 2*D*). Even though the capsule density is higher, oscillations cannot be sustained, due to the smaller span of the colony. These results indicate that the colony behavior depends on the combination of colony size and capsule density.

For insight into the internal dynamics of the colony, we map the concentration fields and spatial distributions of chemical production at various times over a period of oscillation (Fig. 3; also see Movie S1) for the simulation presented in Fig. 2*C*. All capsules oscillate in phase with each other and have similar production rates at any given time. Although chemical production only occurs in the discrete capsules, the concentrations vary smoothly throughout the colony, and the discrete nature of the sources is difficult to discern. The concentration field is approximately radially symmetric and is highest at the center of the colony.

As indicated by the in-phase oscillations of capsules in the colony, our system behaves as a collection of oscillators that undergo synchronization (17–19, 22). In our colony, however, a single capsule in isolation does not exhibit oscillations; oscillations require coupling among many capsules. Notably, similar phenomena have been reported for synchronized glycolytic oscillations in yeast (23).

The above numerical approach is feasible in a limited range of parameter space, because it is computationally demanding to simulate large, 3D domains with each capsule spatially resolved over time scales that are sufficient to evaluate the long-term behavior. To achieve a broad, qualitative understanding of the system, we develop a simpler, coarse-grained model of the colony that allows rapid characterization over a large region of parameter space.

The Continuum Colony Model. To reduce the complexity of our colony model, we replace the collection of discrete capsules with a spatially continuous distribution throughout the volume occupied by the colony. In this continuum model, we do not resolve inhomogeneities on the length scale of the capsule radius but rather consider average effects over macroscopic scales. This simplification is valid assuming the capsules are both small and lie close together relative to the diffusion length of the chemicals. (If the capsules were far apart from each other, then they

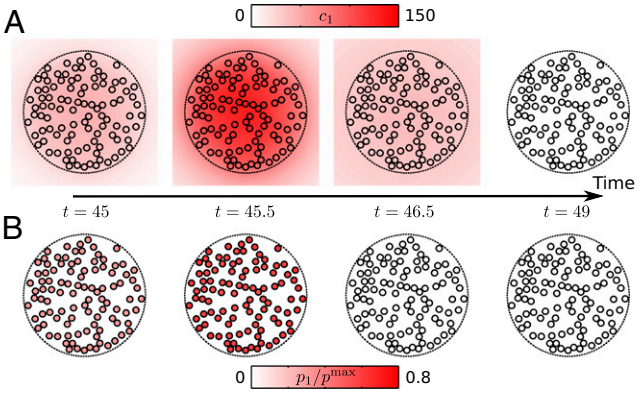

Fig. 3. Concentrations and production rates within an oscillating colony. (*A*) Concentrations of chemical species 1 in the horizontal plane through the center of the colony ($z = 0$) at four times over one period of oscillation. The boundary of the colony is indicated by the dotted line, and positions of capsules are marked by small, open circles. (*B*) Production rates per unit volume normalized by the production capacity p^{max} at the same times as shown in *A*. Production only occurs within capsules. Parameters are $N_{cap} = 100$, $p^{max} = 5{,}000$, and $R_{col} = 1$. This simulation was also used to generate Fig. 2*C*. The time evolution for all three chemicals in this simulation is shown in Movie S1.

would effectively behave independently because the signaling chemicals would decay before diffusing to neighbors.)

The continuum model is described by the same reaction diffusion equations, Eq. **2**, boundary conditions and initial concentrations, Eq. **3**, as the discrete capsule model. The continuum approximation replaces the sum of discrete production terms with a single term,

$$p_j(\mathbf{x},t) = f\left[c_{j-1}(\mathbf{x},t)\right]\Omega_{\mathrm{col}}(\mathbf{x}),$$
$$\Omega_{\mathrm{col}}(\mathbf{x}) = \begin{cases} V_{\mathrm{cap}}\rho_{\mathrm{cap}}, & \text{if } \sqrt{x^2+y^2} \le R_{\mathrm{col}} \\ 0, & \text{otherwise} \end{cases}, \qquad [5]$$

where ρ_{cap} is the number density of capsules and $V_{\mathrm{cap}} = 4\pi R_{\mathrm{cap}}^3/3$ is the volume of a capsule. Hence, the colony indicator function Ω_{col} describes the local volume fraction of capsules. We consider colonies with uniform distributions of capsules so that ρ_{cap} does not vary with position.

We further simplify the model by assuming that the production rates per unit volume are spatially uniform throughout the colony at any given time. This assumption is motivated by observations of in-phase synchronized oscillations of all capsules in our discrete simulations (Fig. 3) and is justified if the inhibitor concentrations are approximately homogeneous throughout the colony. We choose to evaluate the homogeneous production rates based on the chemical concentrations at the center of the colony, denoted by $C_j(t) = c_j(\mathbf{x}=\mathbf{0},t)$. The production term is $p_j(\mathbf{x},t) = f[C_{j-1}(t)]\Omega_{\mathrm{col}}(\mathbf{x})$, and the (homogenized) maximum production rate per unit volume inside the colony is $p_{\mathrm{col}}^{\max} = V_{\mathrm{cap}}\rho_{\mathrm{cap}}p^{\max}$. The model parameters in this coarse-grained description of the capsule colony are R_{col}, $p_{\mathrm{col}}^{\max}$, and n. The parameters describing single, discrete capsules, R_{cap} and $p^{\max}$, can be thought of as fixed while the number of capsules and spacing between capsules are varied to change R_{col} and $p_{\mathrm{col}}^{\max}$.

We first consider the case $n=3$ and vary R_{col} and $p_{\mathrm{col}}^{\max}$ over several orders of magnitude. We use the method of Green's functions (24) to obtain an expression for the solution in a form amenable to stability analysis (see *SI Text* for details). A unique pair of steady-state concentration and production rate (identical for all three species $j=1,2,3$ by symmetry) is found for each set of parameters. The phase map in Fig. 4*A* shows the respective regions of parameter space with linearly stable and unstable steady states. We also performed numerical solution of the reaction–diffusion equations, relaxing the assumption of uniform chemical production (see *SI Text* for details). The simulations were consistent with the uniform colony stability analysis; oscillatory behavior emerges when the steady state is linearly unstable, and steady behavior emerges in the linearly stable regime (Fig. 4*B*). This comparison validates our simplification of considering spatially uniform production rates within the colony.

Noting that the maximum production rate per unit volume $p_{\mathrm{col}}^{\max}$ is proportional to the number density of capsules in the colony, the phase maps shown in Fig. 4 demonstrate that the qualitative behavior of the colony is sensitive to colony radius and capsule density, hallmarks of QS in biological organisms. In particular, small and sparse colonies tend to produce chemicals at low, steady rates, whereas large, dense colonies exhibit high-amplitude oscillatory production of chemicals (23). The transition between these two modes of behavior can be described by approximating the regime boundary with two straight line segments, indicated by dashed lines in Fig. 4*A*. The horizontal line denotes a critical value of the production capacity $p_{\mathrm{col}}^{\max} = p_{\mathrm{crit}}^{\max}$, equivalent to a critical capsule density $\rho_{\mathrm{cap}} = \rho_{\mathrm{crit}}$. For colonies of sufficiently large radius, the precise value of the radius is not important in determining the behavior. Oscillations emerge when the capsule density exceeds a threshold, $\rho_{\mathrm{cap}} > \rho_{\mathrm{crit}}$.

The vertical portion of the transition curve corresponds to a critical colony radius $R_{\mathrm{col}} = R_{\mathrm{crit}}$. In the limit of dense colonies

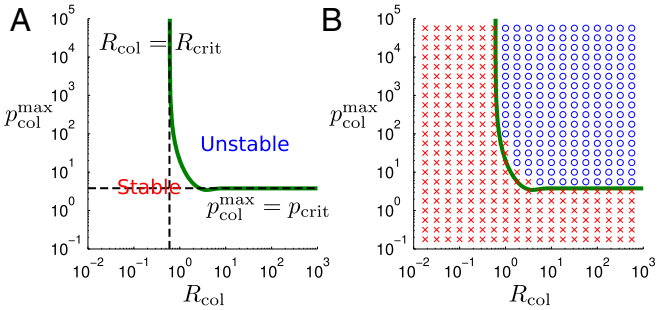

Fig. 4. Phase maps for colonies with Hill coefficient $n = 3$. (*A*) The stability phase map for the continuum colony model assuming uniform production rates. The steady state is linearly stable below the green curve and linearly unstable above the curve. The two dashed lines correspond to the horizontal and vertical asymptotes of the curve respectively. (*B*) A comparison between the theoretical stability map from *A* and simulated behavior of colonies with radially varying production rates (see *Supporting Information* for simulation details). Open circles (blue) mark simulations with sustained oscillatory behavior, and crosses (red) mark simulations that approached steady behavior.

(high $p_{\mathrm{col}}^{\max}$ or ρ_{cap}), the transition from steady to oscillatory behavior occurs when the colony radius exceeds a threshold, $R_{\mathrm{col}} > R_{\mathrm{crit}}$. If either the colony radius or the production capacity is below the threshold, or if both quantities are close to their respective thresholds, then the colony will relax to a steady-state behavior.

The QS characteristics we observe for this colony of synthetic capsules (with Hill coefficient $n=3$) resemble the responses exhibited in biological QS; namely, a certain behavior is activated when the population size and density become sufficiently high. Our repressilator colony system, however, can produce different responses to varying capsule number and density, depending on the choice of the Hill coefficient. In Fig. 5, we overlay the phase map boundaries separating stable and oscillatory regimes for different Hill coefficients $n=2,3,4,5$ (nota bene, the Hill coefficient can take fractional values in both experimental and theoretical systems). The cases $n=4,5$ show, qualitatively, the same QS transition as the $n=3$ case described above. The critical production capacity and the critical colony radius decrease as n increases. Thus, oscillations are more likely in systems with large Hill coefficients.

In the case $n=2$, a qualitatively different phase map boundary is obtained between the oscillatory and steady regimes. As the colony radius increases, oscillations require increasingly high capsule densities. There may be an upper limit to the colony radius beyond which oscillations cannot be sustained at any value of the production capacity, although this asymptotic behavior is not clear from the range of parameter values tested. The shape of the oscillatory regime in Fig. 5 indicates that the $n=2$ repressilator system can function as a "bandpass" filter, allowing oscillations to emerge only within a specific range of R_{col}. Although this functionality may not be common in biological QS, it is useful in engineered systems in providing additional degrees of self-regulation.

The characteristic that oscillations cease as the colony radius increases (for $n=2$) is consistent with previous theoretical studies of well-mixed (homogeneous) repressilator systems (13). Using a system of ordinary differential equations to model the repressilator kinetics without diffusion, it was shown that the $n=2$ case does not exhibit oscillations unless the model is formulated with an additional three chemical species representing mRNA molecules that are involved in the production of proteins by living cells. As our capsule colony becomes larger, the interior becomes less affected by the finite size of the colony and behaves like an infinite, homogeneous system. In this homogeneous limit,

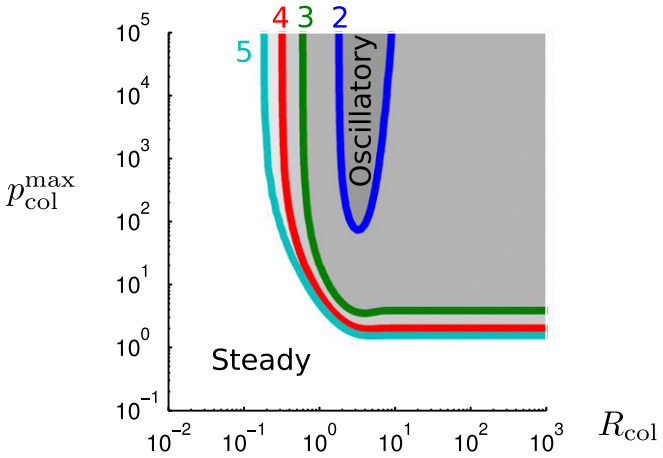

Fig. 5. Phase maps for colonies with various values of Hill coefficient. Boundaries between steady and oscillatory behavior, determined using the continuum colony model with uniform production, are plotted for Hill coefficients n = 2,3,4,5 as labeled. Larger Hill coefficients allow oscillations in larger regions of parameter space.

it was shown (14) that the steady state is always stable for $n \leq 2$ but that a Hopf bifurcation leads to oscillations whenever $n > 2$ and (in our notation) $p_{\mathrm{col}}^{\max} > p_{\mathrm{crit}}^{\max} = r_0^{n+1} + r_0$, where $r_0 = \sqrt[n]{2/(n-2)}$. Table S1 compares this formula for the critical production capacity in well-mixed systems with thresholds obtained numerically in the large colony limit. Our results for large colony sizes agree well with the homogeneous description, but we also demonstrate that diffusion is an important process for small colonies and can lead to chemical oscillations that are otherwise not possible. [In *Supporting Information*, we also compare the periods and amplitudes of oscillation for the well-mixed and heterogeneous systems (Figs. S1 and S2).]

In the above discussion, we focused on analysis of a 2D colony of capsules because this is potentially the simplest arrangement to realize experimentally; unless the fluid and microcapsule mass densities are carefully matched, the microcapsules would naturally settle into a 2D layer in a microfluidic chamber, as in experiments with porous catalytic particles (19). Nevertheless, 3D arrangements of capsules are experimentally possible, as are 1D arrangements in a capillary tube or other channel. It is straightforward to adapt both the discrete and the continuum colony models to determine the behavior in such systems, although numerical solution becomes much slower as the dimensionality increases. In *SI Text*, we present a QS phase map for spherical colonies in unbounded, 3D space (Fig. S3). The results are similar to the 2D case shown in Fig. 5; oscillations are favored by large colony sizes, high production capacities, and large values of the Hill coefficient.

Conclusions

We developed a theoretical model for the chemical activity of a colony of microcapsules that produce and release chemical species. Our approach extends standard mathematical models for reaction kinetics in well-mixed systems to a spatially heterogeneous description by considering capsules to be diffusively coupled, localized sources. Simulations showed that the colonies regulated by the repressilator feedback network exhibited QS behavior. For example, small colonies gave steady, low production of chemicals (off state), whereas large, dense colonies generated large-amplitude oscillations in chemical production rates and concentrations (on state). Using a simplified model, we characterized the dependence of the emergent behavior on model parameters, enabling systems with particular transitions to be designed. For instance, colonies are generally switched on when the colony radius is sufficiently large. With the Hill coefficient $n = 2$, however, it is possible to design colonies that switch off when the radius is large. Such behavior is not possible with the QS networks in bacteria.

The models and simulation techniques we have implemented can be extended and applied to arbitrary regulatory networks to investigate the coordinated behavior in other systems of synthetic or biological cells. Notably, these findings show that QS can emerge from regulatory networks that are not used for QS in biological systems and hence reveal that a variety of feedback loops could enable sensitivity to the number and density of elements in a colony.

Our findings have important implications for designing novel mechanoresponsive materials. In particular, the capsules can be embedded within and chemically linked to a polymer gel, or the enzymes can be directly immobilized in hydrogels (25). Mechanical deformation (extension or compression) can be harnessed to tailor the separation between the capsules and thus create materials that controllably emit oscillatory signals.

In systems of free (unbound) capsules, chemical concentration gradients can cause the capsules to move due to diffusiophoresis, for example. The signaling molecules, or other secreted chemicals, would control the motion of the capsules in addition to regulating reactions. Such systems could display complex self-organizing behavior, as there is bidirectional feedback between the spatial arrangement of capsules and the chemical activity. Previous simulations demonstrated that a group of three capsules, each producing a different component of the repressilator network, could dynamically regulate chemical concentration gradients to induce rapid aggregation of the capsules (24). Applying a similar mechanism for gradient-driven motion of QS capsules could enable large populations to aggregate when the population density locally reaches a critical threshold, mimicking the coordinated aggregation of slime mold cells. It is also possible to envision engineering other collective phenomena, such as oscillating contraction and expansion of colonies, by modifying the diffusiophoretic response of capsules to each chemical species.

Finally, based on recent experimental studies (26–30), we propose potential routes for physically realizing our QS microcapsules. A key component for QS in our system is a regulated production of chemicals. In our model, this is achieved through the repressilator network, which enables self-sustained oscillations under specific conditions. The original realization of the repressilator was based on regulation of a synthetic gene network in living cells (12). The repressilator motif can, however, be implemented in cell-free alternatives, which use biochemical mixtures to execute the regulation scheme (26, 29). In particular, in vitro transcriptional circuits can be systematically assembled to form arbitrary networks in an experimentally simple manner (31); oscillators, including the repressilator, have been successfully constructed using this technique (26, 27).

The three chemical species in the repressilator network are inhibitor species of RNA (26, 27, 31). The kinetics following this mechanism of inhibition were experimentally shown to be approximated by the Hill function, as was assumed in our model (31). The value of the effective Hill coefficient n varied between 3 and 6, depending on controllable experimental conditions (31). Thus, our predictions on variations in the system behavior with changes in n could be tested experimentally.

In addition to the regulated production of chemicals, to experimentally realize our system, we need to enclose the regulating network within microcontainers, while still allowing chemical communication among these containers. Encapsulation of cell-free biochemical networks has been achieved using phospholipid vesicles (30) and water-in-oil microemulsion droplets (27, 29). Certain small molecules used in bacterial QS, such as *N*-(3-oxo-hexanoyl)-L-homoserine lactone, could pass

through vesicle membranes (30) and the oil phase surrounding emulsion droplets (29), thus facilitating intercellular communication. Channel proteins could be used to allow transport of other signaling species across vesicle membranes (32), and stomatocytes with large openings would also freely exchange a wide range of materials with the external fluid (33). Hence, the necessary components for experimentally realizing our system are available.

As an alternative route, the necessary enzymes can be confined in membraneless compartments by complex coacervation (34, 35). Under specific conditions of temperature, pH, and ionic strength, polyelectrolytes can undergo phase separation and form coacervate droplets that are enriched in protein molecules (34). Lacking membranes, signaling species could freely diffuse into and out of the droplets. Intriguingly, the condition dependence of coacervation provides a mechanism for dynamically aggregating and dispersing the enzymes. Because our model indicates that oscillations occur when there is a large, concentrated aggregate of chemical-producing material, we could design systems that oscillate when a certain temperature is reached, for example, and phase separation occurs.

Methods

We use a finite difference approach to numerically solve an approximation to the model described by Eqs. **2**–**4**. The forward-time centered-space scheme is implemented for the temporal and spatial derivatives (36, 37). The computational domain is the 3D box defined by $-L/2 \le x \le L/2$, $-L/2 \le y \le L/2$, $-h/2 \le z \le h/2$. Periodic boundary conditions are used for the x and y boundaries, and impermeable boundary conditions are used for the z boundaries,

$$\begin{aligned} c_j(x=-L/2,y,z,t) &= c_j(x=L/2,y,z,t),\\ c_j(x,y=-L/2,z,t) &= c_j(x,y=L/2,z,t),\\ \left.\frac{\partial c_j}{\partial z}\right|_{z=-h/2} &= \left.\frac{\partial c_j}{\partial z}\right|_{z=h/2} = 0. \end{aligned} \quad [6]$$

Restricting our studies to 2D arrangements of capsules, we consider a thin domain $h = 2R_{cap}$ as shown in Fig. 1. To reduce the influence of the lateral (x, y) periodic boundaries, we place them far away from the colony by setting the domain length $L = 2(R_{col} + \Lambda)$ with $\Lambda = 3$. In nondimensionalized units, the characteristic time required for a chemical to diffuse by a distance Λ is $t_\Lambda = \Lambda^2 = 9$. Over this time, first-order degradation removes $(1 - e^{-t_\Lambda}) = 99.99\%$ of the chemical. Hence, chemical concentrations at the lateral boundaries are negligible, and the periodicity of the computational domain should have little effect on the behavior of the colony.

The domain is discretized using a regular square grid with spacing $\Delta x = 0.02$. The typical grid size is $400 \times 400 \times 5$, for example, for the simulations presented in Fig. 2 *B* and *C*. The time step size used with the finite difference scheme is $\Delta t = 4 \times 10^{-5}$.

The centers of all capsules are confined to the plane $z = 0$. The (x,y) coordinates are chosen randomly from a uniform distribution. The position is rejected and redrawn from the uniform distribution if the capsule would be placed outside the colony ($R_{cap} + \sqrt{x^2 + y^2} > R_{col}$) or if the capsule would overlap a previously accepted capsule placement. At each simulation time step, the chemical production term defined in Eq. **1** is applied to all grid cells within a distance R_{cap} of a capsule center.

ACKNOWLEDGMENTS. This work was supported as part of the Center for Bio-Inspired Energy Science, an Energy Frontier Research Center funded by the U.S. Department of Energy, Office of Science, Basic Energy Sciences under Award DE-SC0000989.

1. Miller MB, Bassler BL (2001) Quorum sensing in bacteria. *Annu Rev Microbiol* 55: 165–199.
2. Goo E, et al. (2012) Bacterial quorum sensing, cooperativity, and anticipation of stationary-phase stress. *Proc Natl Acad Sci USA* 109:19775–19780.
3. Avbelj M, Zupan J, Kranjc L, Raspor P (2015) Quorum-sensing kinetics in *Saccharomyces cerevisiae*: A symphony of ARO genes and aromatic alcohols. *J Agric Food Chem* 63:8544–8550.
4. Sprague GF, Jr, Winans SC (2006) Eukaryotes learn how to count: Quorum sensing by yeast. *Genes Dev* 20:1045–1049.
5. Golé L, Rivière C, Hayakawa Y, Rieu J-P (2011) A quorum-sensing factor in vegetative *Dictyostelium discoideum* cells revealed by quantitative migration analysis. *PLoS One* 6:e26901.
6. Brock DA, Gomer RH (1999) A cell-counting factor regulating structure size in *Dictyostelium*. *Genes Dev* 13:1960–1969.
7. Seeley TD, Visscher PK (2004) Group decision making in nest-site selection by honey bees. *Apidologie (Celle)* 35:101–116.
8. Jayaraman A, Wood TK (2008) Bacterial quorum sensing: signals, circuits, and implications for biofilms and disease. *Annu Rev Biomed Eng* 10:145–167.
9. Dockery JD, Keener JP (2001) A mathematical model for quorum sensing in *Pseudomonas aeruginosa*. *Bull Math Biol* 63:95–116.
10. Melke P, Sahlin P, Levchenko A, Jönsson H (2010) A cell-based model for quorum sensing in heterogeneous bacterial colonies. *PLOS Comput Biol* 6:e1000819.
11. Goryachev AB, Toh DJ, Lee T (2006) Systems analysis of a quorum sensing network: Design constraints imposed by the functional requirements, network topology and kinetic constants. *Biosystems* 83:178–187.
12. Elowitz MB, Leibler S (2000) A synthetic oscillatory network of transcriptional regulators. *Nature* 403:335–338.
13. Loinger A, Biham O (2007) Stochastic simulations of the repressilator circuit. *Phys Rev E Stat Nonlin Soft Matter Phys* 76:051917.
14. Buşe O, Kuznetsov A, Pérez RA (2009) Existence of limit cycles in the repressilator equations. *Int J Bifurcat Chaos* 19:4097–4106.
15. Blossey R, Giuraniuc CV (2008) Mean-field versus stochastic models for transcriptional regulation. *Phys Rev E Stat Nonlin Soft Matter Phys* 78:031909.
16. Müller SC, Mair T, Steinbock O (1998) Traveling waves in yeast extract and in cultures of *Dictyostelium discoideum*. *Biophys Chem* 72:37–47.
17. Kuramoto Y, Yamada T (1976) Pattern formation in oscillatory chemical reactions. *Prog Theor Phys* 56:724–740.
18. Danino T, Mondragón-Palomino O, Tsimring L, Hasty J (2010) A synchronized quorum of genetic clocks. *Nature* 463:326–330.
19. Tinsley MR, Taylor AF, Huang Z, Wang F, Showalter K (2010) Dynamical quorum sensing and synchronization in collections of excitable and oscillatory catalytic particles. *Phys Nonlinear Phenom* 239:785–790.
20. Goutelle S, et al. (2008) The Hill equation: A review of its capabilities in pharmacological modelling. *Fundam Clin Pharmacol* 22:633–648.
21. West SA, Winzer K, Gardner A, Diggle SP (2012) Quorum sensing and the confusion about diffusion. *Trends Microbiol* 20:586–594.
22. Garcia-Ojalvo J, Elowitz MB, Strogatz SH (2004) Modeling a synthetic multicellular clock: Repressilators coupled by quorum sensing. *Proc Natl Acad Sci USA* 101: 10955–10960.
23. De Monte S, d'Ovidio F, Danø S, Sørensen PG (2007) Dynamical quorum sensing: Population density encoded in cellular dynamics. *Proc Natl Acad Sci USA* 104: 18377–18381.
24. Shum H, Yashin VV, Balazs AC (2015) Self-assembly of microcapsules regulated via the repressilator signaling network. *Soft Matter* 11:3542–3549.
25. Hwang ET, Gu MB (2013) Enzyme stabilization by nano/microsized hybrid materials. *Eng Life Sci* 13:49–61.
26. Kim J, Winfree E (2011) Synthetic in vitro transcriptional oscillators. *Mol Syst Biol* 7: 465.
27. Weitz M, et al. (2014) Diversity in the dynamical behaviour of a compartmentalized programmable biochemical oscillator. *Nat Chem* 6:295–302.
28. Semenov SN, et al. (2015) Rational design of functional and tunable oscillating enzymatic networks. *Nat Chem* 7:160–165.
29. Schwarz-Schilling M, Aufinger L, Mückl A, Simmel FC (2016) Chemical communication between bacteria and cell-free gene expression systems within linear chains of emulsion droplets. *Integr Biol* 8:564–570.
30. Lentini R, et al. (2017) Two-way chemical communication between artificial and natural cells. *ACS Cent Sci* 3:117–123.
31. Kim J, White KS, Winfree E (2006) Construction of an in vitro bistable circuit from synthetic transcriptional switches. *Mol Syst Biol* 2:68.
32. Palivan CG, Fischer-Onaca O, Delcea M, Itel F, Meier W (2012) Protein-polymer nanoreactors for medical applications. *Chem Soc Rev* 41:2800–2823.
33. Nijemeisland M, Abdelmohsen LKEA, Huck WTS, Wilson DA, van Hest JCM (2016) A compartmentalized out-of-equilibrium enzymatic reaction network for sustained autonomous movement. *ACS Cent Sci* 2:843–849.
34. Lindhoud S, Claessens MMAE (2016) Accumulation of small protein molecules in a macroscopic complex coacervate. *Soft Matter* 12:408–413.
35. Aumiller WM, Jr, Pir Cakmak F, Davis BW, Keating CD (2016) RNA-based coacervates as a model for membraneless organelles: formation, properties, and interfacial liposome assembly. *Langmuir* 32:10042–10053.
36. Özişik MN (1994) *Finite Difference Methods in Heat Transfer* (CRC, Boca Raton, FL).
37. Thomas JW (1995) *Numerical Partial Differential Equations: Finite Difference Methods* (Springer, New York).